C15

**Single channel properties of mature rat glycine receptors from spinal motoneurones**

M. Beato and L.G. Sivilotti

*Pharmacology, University College London, London, UK*

Heteromeric $\alpha1\beta$ channels are the main isoform of glycine receptors (GlyRs) in adult mammalian neurones. We have recently formulated a detailed activation mechanism that accounts for the single-channel properties of recombinant $\alpha1\beta$ GlyRs (1). The aim of the present experiments is to determine whether the same kinetic scheme can provide a satisfactory description of the behaviour of native GlyRs. The lumbar spinal cord was dissected rapidly post mortem from juvenile rats (P12-15) and slices (350 μm thick) cut using a vibratome. Single channel recordings were performed from motoneurones (visually identified by their morphology and location in the ventral horn) in the cell-attached or in the outside-out configuration.

Surprisingly, only a small minority of cell-attached patches contained glycine-activated channels (14/~1200 patches). On the contrary, GlyRs were observed in the majority of outside-out patches, possibly because outside-out patches have a much larger surface area. Channel properties were found to be substantially different in the two configurations.

In cell-attached mode, only one current amplitude was observed in the presence of 30, 100 or 1000 μM glycine. Native GlyR amplitudes varied from patch to patch (range 1.8-3 pA) reflecting differences in the intracellular chloride concentration. Nevertheless, the single channel conductance (estimated applying a 1s voltage ramp) was similar to that measured in cell-attached experiments from recombinant heteromeric GlyRs (2) (41±1 pS (n=14) vs 39±1 pS (n=5); all data expressed as mean±S.E.M.).

On the other hand, in excised patches, glycine channels opened to several different amplitudes (typically 2 or 3). Average chord conductance values were similar for GlyRs from spinal motoneurones (28, 38 and 46 pS, n=7, 1 mM glycine) and for recombinant $\alpha1\beta$ channels from HEK293 cells (27, 34 and 45 pS, n=9).

In our investigation of the kinetic properties of native glycine channels, we focused on the cell-attached configuration, as this is closer to physiological conditions. Thus we selected two cell-attached experiments in which enough transitions were recorded and the signal to noise ratio allowed detection of transitions as short as 30 μs. At 1 mM glycine, the open period distribution was described by a single exponential ($\tau$=7.0±0.3 ms) and 98±1% of the shut times distribution is described by an exponential with time constant of 11 μs, in good agreement with values from recombinant $\alpha1\beta$ GlyRs.

The gating rates for the fully liganded native receptor, calculated from maximum likelihood fitting (HJCFIT program, http://www.ucl.ac.uk/Pharmacology/dc.html), were found to be similar to those estimated for recombinant receptors (1).

This suggests that the gating behaviour of fully liganded native channels closely resembles that of recombinant $\alpha1\beta$ glycine receptors.

Burzomato et al. (2004). J Neurosci 24, 10924-10940.

Burzomato et al. (2003). Receptors and channels 9, 353-361.

This work was supported by the MRC, Wellcome Trust and Royal Society.

*Where applicable, the authors confirm that the experiments described here conform with the Physiological Society ethical requirements.*

C16

**Dephosphorylation by protein phosphatase 1 reduces the single-channel conductance of recombinant GluR1 AMPARs**

I.D. Coombs, M. Farrant and S.G. Cull-Candy

*Pharmacology, UCL, London, UK*

AMPA-type receptors (AMPARs) are responsible for the fast component of glutamate mediated synaptic excitation in the CNS. Four receptor subunits exist (GluR1-4), with receptor heterogeneity being achieved through RNA editing, alternative splicing and heteromerization. Modulation of AMPARs underlies various forms of plasticity including long-term potentiation (LTP) and depression (LTD). GluR1-containing AMPARs are found in many cell populations that display LTP, including CA1 pyramidal cells of the hippocampus. Phosphorylation of two sites within the C-terminus of GluR1 can modulate either the single-channel conductance (Ser831; Derkach et al. 1999) or the peak channel open-probability (Ser845; Banke et al. 2000). Protein kinase A (PKA) and calcineurin, respectively, phosphorylate and dephosphorylate Ser845. Calcium/calmodulin-dependent protein kinase II (CaMKII) phosphorylates Ser831. We have now identified a phosphatase responsible for dephosphorylating this site, and have examined its effects on channel properties.

We expressed recombinant AMPARs in tsA cells (a modified HEK293 cell line) transiently transfected with GluR1 and constitutively active forms of both CaMKII and Protein Phosphatase 1 (PP1). GluR1 responses were evoked by fast application of 10mM glutamate to outside-out patches. Unexpectedly, our initial experiments failed to demonstrate a potentiation of homomeric GluR1 AMPAR-currents following co-expression with CaMKII. However, following co-expression with PP1, the channel conductance decreased suggesting that an endogenous kinase (possibly a PKC isoform), maintains phosphorylation of GluR1 subunits in our conditions. GluR1 responses were analysed by non-stationary noise analysis, yielding a weighted-mean single-channel conductance of 23.1 ± 1.9pS (n = 7). This conductance was not significantly altered by CaMKII (25.8 ± 2.6pS; n = 6) but was decreased by PP1 (15.5 ± 1.2pS; n = 10, $P < 0.01$ vs control and CaMKII).

Our experiments have identified an experimental system in which GluR1 is constitutively phosphorylated. In these conditions the phosphatase PP1 is capable of down-regulating GluR1 responses by reducing channel conductance. Mice lacking PP1 show improved abilities in various tests of memory (Genoux et al. 2002). Thus, activation or inhibition of PP1 represents a potential method for induction of plasticity changes.

Banke TG, Bowie D, Lee H, Huganir RL, Schousboe A & Traynelis SF (2000). J Neuroscience 20, 89-102.

Derkach V, Barria A & Soderling TR (1999). PNAS 96, 3269-3274.

Genoux D, Haditsch U, Knobloch M, Michalon A, Storm D & Mansuy IM (2002). Nature 418, 970-975.

This work is supported by the Wellcome Trust (S.G.C.-C. and MF), and a Royal Society-Wolfson Research Award (S.G.C.-C.).

*Where applicable, the authors confirm that the experiments described here conform with the Physiological Society ethical requirements.*

C17

## Glycine potency among rat recombinant *N*-methyl-D-aspartate receptor subtypes is influenced by the S2 glutamate binding region of the NR2 subunit

P.E. Chen[1], K. Erreger[2], M. Livesey[1], S.F. Traynelis[3] and D.J. Wyllie[1]

*[1]Neuroscience, University of Edinburgh, Edinburgh, UK, [2]Molecular Physiology and Biophysics, Vanderbilt University, Nashville, TN, USA and [3]Pharmacology, Emory University, Atlanta, GA, USA*

The NMDA-subtype of ionotropic glutamate receptor (NMDAR) is comprised of both NR1 and NR2 subunits. The NR1 subunit binds the NMDAR co-agonist glycine, while glutamate binds to NR2 subunits of which there are four types (A–D). The binding sites for either glycine or glutamate are formed by two regions within each subunit (S1 and S2) (see Chen & Wyllie, 2006). It is known that glycine potency varies between recombinant NMDARs containing different NR2 subunits, for example glycine potencies of NR2A- or NR2D-containing NMDARs differ by an order of magnitude. Therefore this heterogeneity in glycine potency must be specified by the particular NR2 subunit within the NMDAR complex since the glycine-binding NR1 subunit is ubiquitous. To investigate the molecular mechanisms underlying this, we generated a number of chimaeric NR2A/NR2D subunits with exchanges in the S1 and S2 domains. NR2 chimaeras were coexpressed with NR1 in *Xenopus* oocytes and agonist-evoked inward currents examined. In the presence of saturating concentrations of glutamate, glycine concentration-response curves generated from NMDARs containing NR2A subunits including the NR2D S1 region gave mean glycine $EC_{50}$ values ($EC_{50}$=1.02 ± 0.06 μM) similar to wildtype NR2A-containing receptors ($EC_{50}$=1.29 ± 0.08 μM). However, oocytes expressing receptors containing NR2A subunits including the NR2D S2 region ($EC_{50}$=219 ± 13 nM) or both NR2D S1 and S2 regions ($EC_{50}$=233 ± 10 nM) produced glycine potencies similar to those seen in wildtype NR2D-containing NMDARs ($EC_{50}$=129 ± 7 nM) (n=13-26 oocytes per experiment). These changes in glycine potency occurred in the absence of any obvious alteration in competitive antagonist affinity at the glycine site, as judged by Schild analysis. This suggests that the variation in glycine potency among NMDAR subtypes may be caused by allosteric interactions between the NR1 and NR2 binding domains rather than by inducing a direct structural change in the NR1-glycine binding site.

Chen PE & Wyllie DJA (2006). *Br J Pharmacol* DOI: 10.1038/sj.bjp.0706689.

Supported by the BBSRC and NIH.

*Where applicable, the authors confirm that the experiments described here conform with the Physiological Society ethical requirements.*

C18

## Determination of equilibrium constants for NVP-AAM077 acting at rat recombinant NR1/NR2A and NR1/NR2B NMDA receptors: implications for studies of synaptic transmission

P.A. Frizelle, P.E. Chen and D.J. Wyllie

*Neuroscience, University of Edinburgh, Edinburgh, UK*

We have quantified the effects of the NMDA receptor antagonist, (R)-[(S)-1-(4-bromo-phenyl)-ethylamino]-(2,3-dioxo-1,2,3,4-tetrahydroquinoxalin-5-yl)-methyl]-phosphonic acid (NVP-AAM077; (1)), at rat recombinant NR1/NR2A and NR1/NR2B NMDA receptors expressed in *Xenopus laevis* oocytes. We observed no difference in the steady-state levels of inhibition produced by NVP-AAM077 when it was either pre-applied or co-applied with glutamate. The $IC_{50}$ values for NVP-AAM077 acting at NR1/NR2A NMDA receptors were, as expected, dependent on the glutamate concentration used to evoke responses being 31 ± 2 nM (n=12; with glutamate at its $EC_{50}$ concentration) and 214 ± 10 nM (n=10; at 10-times the $EC_{50}$ concentration). Schild analysis confirmed that the antagonism produced by NVP-AAM077 at NR1/NR2A NMDA receptors was competitive and gave an estimate of its equilibrium constant ($K_B$) of 15 ± 2 nM (n=9). Furthermore, Schild analysis of an NMDA receptor carrying a threonine to alanine point mutation in the NR2A ligand-binding site indicated that NVP-AAM077 still acted in a competitive manner but with its $K_B$ increased by around 15-fold (220 ± 10 nM; n=8). At NR1/NR2B NMDA receptors, NVP-AAM077 displayed reduced potency. An $IC_{50}$ value of 215 ± 13 nM (n=14) was obtained in the presence of the $EC_{50}$ concentration of glutamate (1.5 μM), while a value of 2.2 ± 0.14 μM (n=8) was obtained with higher (15 μM) glutamate concentrations. Schild analysis gave a $K_B$ for NVP-AAM077 at NR2B-containing receptors of 78 ± 3 nM. In the case of both NR1/NR2A and NR1/NR2B NMDA receptors the antagonism by NVP-AAM077 was surmountable by increasing the concentration of glutamate used to evoke responses. Thus while our data show that NVP-AAM077 is indeed a more potent antagonist at NR1/NR2A compared to NR1/NR2B NMDA receptors the extent of its selectivity is only around 5-fold. Using a kinetic scheme (2) to model 'synaptic-like' activation (10 mM pulse of glutamate for 1 ms) of NMDA receptors we show that the difference in the equilibrium constants for NVP-AAM077 is not sufficient to discriminate selectively between NR2A-containing or NR2B-containing NMDA receptors and that substantial block of both NMDA receptor subtypes occurs with concentrations of NVP-AAM077 commonly used in neurophysiological studies. Indeed the potency of NVP-AAM077 at both NR1/NR2A and NR1/NR2B NMDA receptors is such that on a 'synaptic time-scale' this antagonist can be considered to act in an irreversible manner.

Auberson *et al.* (2002). *Bioorg Med Chem Lett* **12**, 1099–1102.

Erreger *et al.* (2005). *J Physiol* **563**, 345-358.

We thank Dr Yves Auberson (Novartis Institutes for Biomedical Research, Basel, Switzerland) for the generous gift of NVP-AAM077 and Dr Stephen Traynelis (Emory University, Atlanta, GA) for supplying us with NR2B cDNA. Supported by a grant from the BBSRC (BB/D001978/1).

*Where applicable, the authors confirm that the experiments described here conform with the Physiological Society ethical requirements.*

C34

## Lysophospholipids activate a temperature-sensitive TRPM8 channel via a iPLA$_2$–dependent mechanism

A.V. Zholos[2], G. Bidaux[1], F. Vanden Abeele[1], R. Skryma[1] and N. Prevarskaya[1]

*[1]Laboratoire de Physiologie Cellulaire, INSERM U800, USTL, Villeneuve d'Ascq, France and [2]Physiology, Queen's University Belfast, School of Medicine and Dentistry, Belfast, UK*

TRP cation channels are increasingly recognized as membrane 'coincidence detectors' of a number of activator stimuli. Using patch-clamp techniques we have investigated the effects of thapsigargin (TG, 1 μM) and common phospholipids - lysophosphatidylcholine (LPC, 10 μM) and lysophosphatidylinositol (LPI, 10 μM) on the gating of TRPM8 channel, which was cloned from human prostate and stably expressed in HEK-293 cells. The expressed channel protein behaved as a 'classical' cold receptor (e.g. activation by depolarization, cold, menthol and icilin). In the cell-attached configuration cation channel conductance was 73.8±3.6 pS (n=15); its open probability (NPo) was increased upon cooling ($t_{1/2}$=26.6±0.9°C, n=5) from NPo=0.01±0.005 at 37°C (n=6) to NPo=0.26±0.05 at 20°C (n=15) at 80 or 100 mV. Furthermore, NPo voltage dependence was similar to that of cold- or menthol-induced whole-cell current. Thus, we have identified the 74 pS channel activity as a functional counterpart of the expressed TRPM8 protein. Strikingly, channel activity was also potentiated by TG in a time-dependent manner (NPo was 0.12±0.02, 0.46±0.11 and 1.37±0.18 in control, 2 and 10 min after TG application, respectively; n=10). Since iPLA$_2$, a $Ca^{2+}$-independent cytosolic enzyme which produces an array of lysophospholipids, is up-regulated by $Ca^{2+}$ store depletion (Smani et al. 2004) we next tested its possible involvement in TRPM8 activation. The effect of TG on TRPM8 activity was abolished following treatment with the iPLA$_2$ blocker bromoenol lactone. Testing two main iPLA$_2$ products, LPC and LPI, on single channel gating in inside-out patches revealed the underlying channel mechanisms. Channel activity was strongly reduced upon patch excision (4.6±0.7-fold in cell-attached vs. inside-out, n=13) but application of either LPC or LPI to the cytoplasmic side not only restored the activity (as was the case for PIP$_2$ action, Liu & Qin, 2005) but significantly increased NPo (from 0.03±0.01 in control to 0.20±0.09 or 0.93±0.33 with LPC or LPI, respectively; n=5-7). This potentiating effect was associated with the appearance of long channel openings which were also seen during the TG action. These long openings with the mean dwell time of 7.9±2.4 ms and relative contribution of 39±9% (n=7) generated >90% of the mean current. In contrast, in control channel openings were brief (0.48±0.03 ms at 80 mV) while longer openings were only occasionally observed at a very strong depolarization (2.92±1.44 ms, 1.3% contribution at 120 mV in 3 out of 12 patches). Even after menthol application their contribution was only 6±4% although they became more readily detectable (6/6 patches). Thus, we found that physiologically relevant phospholipids can stabilize open conformation of TRPM8 channel far better than other known activating factors.

Smani T et al. (2004). Nat Cell Biol 6, 113-120.

Liu B & Qin F (2005). J Neurosci 25, 1674-1681.

Supported by the Ligue Contre le Cancer and INSERM, France.

*Where applicable, the authors confirm that the experiments described here conform with the Physiological Society ethical requirements.*

C35

## Inhibitory interaction between activated TRPV1 and P2X$_3$ receptors

B.F. King[1], M. Liu[2], A. Townsend-Nicholson[3] and G. Burnstock[2]

*[1]Physiology, UCL, London, UK, [2]Anatomy & Developmental Biology, UCL, London, UK and [3]Biochemistry & Molecular Biology, UCL, London, UK*

ATP-activated P2X$_2$ and P2X$_{2/3}$ receptors mediate slow inward currents in a subset of rat dorsal root sensory neurons (Liu *et al.* 2000) and, in those cells, are inhibited by vanilloid (TRPV1) receptors activated tonically by capsaicin (0.5 μM) (Piper & Docherty, 2000). Here, we identify another inhibitory action of TRPV1 receptors, when activated transiently by capsaicin (0.3-10 μM), on ATP-gated P2X$_3$ receptors which mediate fast inward currents in sensory neurons.

Rat isoforms of TRPV1 and P2X$_3$ receptors were expressed alone, or together, in defolliculated *Xenopus* oocytes and studied under voltage clamp conditions (Axoclamp 2B amplifier; headstage configuration: ME1, x1LU; ME2, x10MGU; input range, ±13 μA). To avoid saturating the current-following headstage, receptor expression levels were kept low by injecting small volumes (20-40 nl) of complementary RNA (1 mg ml$^{-1}$) into oocytes, and the amplitude of evoked currents also kept low (1-2 μA) by holding cells at -30 mV.

With P2X$_3$ receptors alone, rapidly inactivating and pH-insensitive inward currents were evoked by ATP ($EC_{50}$, 1.3±0.3 μM; mean ± SEM, n = 6). ATP potency was unaltered (1.2±0.4 μM; n = 6) by the presence of capsaicin (10 μM) which was not an agonist. With TRPV1 receptors alone, slowly inactivating and pH-sensitive inward currents were evoked by capsaicin ($EC_{50}$, 0.86±0.07 μM; n = 6) and its potency was unaffected (0.88±0.05 μM; n = 6) by the presence of ATP (10 μM) which was not an agonist. With TRPV1 and P2X$_3$ receptor coexpression, the simultaneous activation of both sets of ion channels produced independent responses seemingly unaffected by the activation of the other ion channel population. However, the prior activation of TRPV1 receptors led to a time- and amplitude-dependent inhibition of ATP responses at P2X$_3$ receptors. Inhibition of ATP responses was characterised by a reduction (69±2.3%, n = 5) in agonist efficacy without altering its potency. Inhibition was dependent of extracellular pH, since acidification potentiated capsaicin responses. Similar to the case of P2X$_2$/P2X$_{2/3}$ receptor inhibition (Piper & Docherty, 2000), the inhibitory action of TRPV1 receptors on P2X$_3$ receptors was also dependent on extracellular $Ca^{2+}$ ions. Inhibition was independent of the holding potential in voltage clamp experiments. The prior activation of P2X$_3$ receptors did not affect the amplitude of capsaicin responses.

The observed inhibition of P2X$_3$ receptors by TRPV1 receptors joins a growing list of examples where P2X purinoceptors are affected by non-purinergic ion channels, and occasionally *vice versa*. This particular example draws attention to a therapeutic regulatory interdependence between these ion channels in sen-

sory neurons, since TRPV1 receptor activation by either heat or another stimulus may down-regulate purinergic signalling via $P2X_3$ (and $P2X_{2/3}$) receptors in nociceptive sensory neurons.

Liu M *et al.* (2000). *J Pharm Exp Therap* **296**, 1043-1050.

Piper AS & Docherty RJ (2000). *J Physiol* **523**, 685-696.

*Where applicable, the authors confirm that the experiments described here conform with the Physiological Society ethical requirements.*

---

C36

**Regulation of N-type calcium channel transcript stability by the stargazin-related protein gamma 7**

L. Ferron[1], D.J. Cox[1], J. Leroy[1], K.M. Page[1], M. Nieto-Rostro[1], S. Bolsover[2], A.J. Butcher[1], A. Davies[1], P. Sellaturay[1], W.S. Pratt[1], F.J. Moss[1] and A.C. Dolphin[1]

*[1]Department of Pharmacology, University College London, London, UK and [2]Department of Physiology, University College London, London, UK*

The role of the novel putative stargazin-like γ-subunits in relation to voltage-gated calcium channel function is controversial. We have previously cloned a member of this family, γ7, and found that it markedly reduced functional expression of $Ca_V2.2$ channels. Here we have identified the novel mechanism for this suppression: it results from a 2-fold increase in the $Ca_V2.2$ mRNA degradation rate. After 9 hours with Actinomycin D, rabbit $Ca_V2.2$ mRNA in Xenopus ooytes is reduced by $54.2 \pm 14\%$ under control conditions and by $88.1 \pm 3.6\%$ in the presence of human γ7, n = 11 and 7, respectively (mean±SEM, $P<0.05$, Student's t test). The half-life of $Ca_V2.2$ mRNA was then estimated to be 7.8 h under control conditions and 3.5 h in the presence of γ7. This process regulates the physiological level of $Ca_V2.2$ transcripts, since knockdown of endogenous γ7 with short hairpin RNA constructs in the neuron-like PC12 cell line markedly increased their endogenous $Ca_V2.2$ mRNA level. Physiologically, γ7 mRNA is down-regulated following differentiation of these cells. As the removal of the cytoplasmic C-terminus of γ7 induces the loss of function of γ7, this part of the protein is essential for all its effects. The RNA binding-protein hnRNPA2 is an endogenous binding partner determined by immunoprecipitation and proteomic identification. $Ca_V2.2$ mRNA binds to hnRNPA2 via its A2RE sequences. Our results support the hypothesis that $Ca_V2.2$ mRNA is targeted for degradation by γ7, via binding to hnRNPA2.

*Where applicable, the authors confirm that the experiments described here conform with the Physiological Society ethical requirements.*

PC22

## Sites of neurosteroid action on $GABA_A$ receptors

A.M. Hosie, M.E. Wilkins, H.M. da Silva and T.G. Smart

*Pharmacology, UCL, London, UK*

The neurosteroids, allopreganolone (ALLOP) and tetrahydrodeoxycorticosterone (THDOC), are potent endogenous modulators of mammalian $GABA_A$ receptors.

Determining the physiological roles of steroid modulation has been hampered by a lack of antagonists that selectively prevent steroid binding to specific $GABA_A$ receptor isoforms. To circumvent this problem, we have identified the sites of neurosteroid action on $GABA_A$ receptors to allow the generation of transgenic animals where specific $GABA_A$ receptor isoforms are rendered insensitive to neurosteroids.

ALLOP and THDOC have two distinct effects on mammalian $GABA_A$ receptor function: potentiation of GABA responses, and in the absence of agonist, they can directly activate the receptor. By contrast, insect GABA receptors are virtually insensitive to ALLOP suggesting that they lack one or more critical components of the steroid binding site(s). After reviewing known steroid binding sites in other proteins, these components are likely to be polar residues that can form hydrogen-bonds with the steroid's oxygen moieties. By systematically replacing polar residues in the transmembrane (TM) domains of murine $\alpha1$ and $\beta2$ $GABA_A$ receptor subunits with the hydrophobic side chains found in the Drosophila GABA receptor subunit, RDL, we have identified critical determinants of steroid action on $GABA_A$ receptors. Receptors were expressed as $\alpha1\beta2\gamma2S$ constructs in HEK293 cells and their pharmacology determined under voltage-clamp at -40 mV, using whole-cell patch-clamp electrophysiology.

Residues T237 and Q242 in the first TM domain of the $\alpha1$ subunit were found to be important for steroid activation and modulation of $GABA_A$ receptors, respectively. From dose-response curve analyses, replacing T237 with other polar side chains supported high potency steroid activation (THDOC $EC_{50}$: wild-type, 1609 ± 637 nM; $\alpha$T237S $\beta\gamma$, 1220 ± 383 nM, P>0.05, t test, n = 5), whereas replacement with hydrophobic residues abolished steroid activation ($\alpha$T237V and $\alpha$T237I, $EC_{50}$s > 20 μM, the limit of solubility). All T237 mutants tested had no effect on the potentiating actions of ALLOP or THDOC.

Replacement of Q242 with polar side chains supported high potency steroid potentiation of $EC_{10}$ GABA responses (THDOC $EC_{50}$: wild-type, 282 ± 47 nM; Q242H: 202 ± 64 nM (P>0.05), Q242S: 1109 ± 58 nM (P<0.05) n = 7) whereas hydrophobic substitutions abolished steroid potentiation at concentrations up to 10 μM. The effects of these mutations were specific to neurosteroids and did not affect the actions of three distinct classes of $GABA_A$ receptor modulators (10 nM-1 μM diazepam; 1–50 μM pentobaritone or 300 nM-100 μM mefenamic acid).

These data are consistent with T237 and Q242 contributing to two distinct neurosteroid binding sites on $GABA_A$ receptor $\alpha$ subunits and provide a structural basis from which to generate transgenic animals with neurosteroid-insensitive $GABA_A$ receptors.

This work is supported by the MRC.

*Where applicable, the authors confirm that the experiments described here conform with the Physiological Society ethical requirements.*

PC23

## Association of stromal interaction molecule 1 (STIM1) with human transient receptor potential channel 1 (hTRPC1) regulated by the filling state of the $Ca^{2+}$ stores in human platelets

J.J. Lopez[1], P.C. Redondo[2], J.A. Pariente[1], G.M. Salido[1] and J.A. Rosado[1]

*[1]Department of Physiology, University of Extremadura, Caceres, Extremadura, Spain and [2]Department of Physiology, Development and Neuroscience, University of Cambridge, Cambridge, UK*

Store-operated $Ca^{2+}$ entry (SOCE), a process activated by depletion of intracellular $Ca^{2+}$ stores, is a major pathway for $Ca^{2+}$ influx in non-excitable cells. $Ca^{2+}$ store depletion in platelets results in de novo coupling of the type II inositol 1,4,5-trisphosphate receptor ($IP_3RII$) to the $Ca^{2+}$ entry channel hTRPC1 (Rosado & Sage, 2000), an event supported by remodelling of the actin cytoskeleton (Rosado & Sage, 2001). Recently, stromal interaction molecules (STIMs) have been identified as intraluminal $Ca^{2+}$ sensor proteins involved in the regulation of SOCE (Liou *et al.* 2005; Zhang *et al.* 2005). Here we have investigated the interaction of STIM1 with hTRPC1 and its regulation by the actin cytoskeleton upon depletion of the $Ca^{2+}$ stores in human platelets.

Blood was drawn from healthy, drug free volunteers. Cytoskeletal association of STIM1 in platelets was determined by Western blotting and interaction between STIM1 and hTRPC1 was investigated by co-immunoprecipitation as described previously (Rosado & Sage, 2000). Determination of cell surface expression of STIM1 was performed by immunocytochemistry.

Co-immunoprecipitation experiments indicated that endogenously expressed hTRPC1 interacts with STIM1 in resting platelets suspended in a medium containing 200 μM $Ca^{2+}$ or in a $Ca^{2+}$-free medium. Depletion of the intracellular $Ca^{2+}$ stores, by treatment for 3 min with thapsigargin (TG; 1 μM) in combination with ionomycin (Iono; 50 nM), significantly enhanced the association of STIM1 with hTRPC1 to 153% of control, both in the absence and presence of extracellular $Ca^{2+}$ ($p<0.05$; Student's t test; $n$=8). Similar results were obtained in BAPTA-loaded cells, suggesting that an increase in cytosolic free $Ca^{2+}$ concentration ($[Ca^{2+}]_c$) is not required for the association of STIM1 with hTRPC1. Treatment with TG + Iono increased STIM1 cell surface localization to 250% of control ($p<0.05$; $n$=6).

A small amount of STIM1 (6%) was found to be associated with the cytoskeletal fraction in resting platelets. Cytoskeletal association was significantly increased after treatment with TG + Iono to 195% of control ($p<0.05$). Platelet treatment for 40 min with 10 μM cytochalasin D, to prevent actin filament polymerization (Rosado & Sage, 2001), significantly reduced the association of STIM1 with hTRPC1 in resting platelets by 80 % and abolished the enhanced interaction between STIM1 and hTRPC1 induced by TG + Iono ($p<0.05$; $n$=6).

Our results indicate that $Ca^{2+}$ store depletion stimulates rapid STIM1 surface expression and association with hTRPC1 independently of rises $[Ca^{2+}]_c$. These events require the support of the actin cytoskeleton and are compatible with membrane trafficking underlying de novo coupling of $IP_3RII$ to hTRPC1.

Liou J, Kim ML, Heo WD, Jones JT, Myers JW, Ferrell JE Jr & Meyer T (2005). Curr Biol 15, 1235-1241.

Rosado JA & Sage SO (2000). Biochem J 350, 631-635.

Rosado JA & Sage SO (2001). Biochem J 356, 191-198.

Zhang SL, Yu Y, Roos J, Kozak JA, Deerinck TJ, Ellisman MH, Stauderman KA & Cahalan MD (2005). Nature 437, 902-905.

*Where applicable, the authors confirm that the experiments described here conform with the Physiological Society ethical requirements.*

PC24

## The putative pore-forming region of mammalian CLIC (chloride intracellular channel) proteins

H. Singh and R.H. Ashley

*CIP, Biomedical Sciences, University of Edinburgh, Edinburgh, UK*

CLICs are ubiquitous but controversial ion channel proteins that often coexist in soluble and integral membrane forms (1). Although their roles remain unclear, the *C. elegans* CLIC-like protein exc-4 appears to be essential for intracellular vesicle fusion (2), supporting the idea that CLICs contribute to charge-compensating intracellular anion channels. Soluble CLICs are structurally similar to Ω-type glutathione-S-transferases (3), but the structure of the membrane proteins remains elusive.

Soluble, recombinant, human CLIC1 and rat brain CLIC4 (p64H1) were incorporated into planar lipid bilayers. CLIC1 formed channels of 38 ± 3 pS (mean ± SD, n = 23) under strongly-reducing conditions with 500 mM KCl on the 'cytosolic' side and 50 mM KCl on the opposite ('luminal') side, while CLIC4 formed channels of 10.3 ± 1.0 pS (mean ± SD, n = 15). CLIC1 was mildly anion selective (Pa/Pc = 1.4 ± 0.25 n = 23), whereas CLIC4 (despite its name) was mildly cation-selective (Pa/Pc (relative permeability of anions vs cations) = 0.54 ± 0.09, n = 15, P <0.01 by t test). In glutathione buffers both channels showed a 'smooth' reduction in amplitude on oxidation, previously attributed (in CLIC1) to unstable disulphide bond formation between pairs of membrane subunits (4).

We identified a putative pore-forming region based on hydropathy plots, protease digestion studies, the sidedness of the N- and C-termini, and exc-4 truncation studies, and tested the idea that CLIC channels contain at least 4 subunits each with a single transmembrane domain (TMD). In this simple model, the luminal (or external) side of each subunit contains a single cysteine residue located just before the putative pore entrance. Consistent with these ideas, truncated proteins comprising the first 58 residues of CLIC1, or the first 61 residues of CLIC4 (sufficient in each case to contain the putative TMD), autoinserted into bilayers to form redox-sensitive ion channels. 0.2 mM thiol-reactive dithiobis-nitrobenzoic acid (DTNB) blocked both the full-length and truncated channels, but only from the luminal side. The truncated proteins showed a reduced conductance, and were non-selective between anions and cations. The very poor ionic selectivity of full-length 'CLIC' channels may be conferred by the channel vestibules rather than the (very similar) residues lining the putative pore, and charged residues in the vestibule may 'concentrate' permeant ions and increase the single-channel conductance (cf (5)).

Ashley RH (2003). Mol Membr Biol 20, 1-11.

Berry KL et al. (2003). Science 302, 2134-2137.

Harrop SJ et al. (2001). J Biol Chem 276, 44993-5000.

Singh H & Ashley RH (2006). Biophys J 90, 1628-1638.

Brelidze TI et al. (2003). Proc Natl Acad Sci USA 100, 9017-9022.

Supported by the College of Medicine and Veterinary Medicine (H.S.) and by an ORS award (H.S.).

*Where applicable, the authors confirm that the experiments described here conform with the Physiological Society ethical requirements.*

PC26

## Oestrogen regulation of voltage-gated $Na^+$ channel expression and activity in the MDA-MB-231 human breast cancer cell line transfected with alpha-oestrogen receptor

I. Ozerlat[1], S.P. Fraser[1], J.K. Diss[2], Y.A. Ushkaryov[1], D.S. Latchman[2] and M.B. Djamgoz[1]

*[1]Division of Cell and Molecular Biology, Imperial College London, London, UK and [2]Medical Molecular Biology Unit, Institute of Child Health, London, UK*

Oestrogen is well known to be involved in development and progression of human breast cancer (BCa) but problems remain in understanding its modes of action and maximizing its therapeutic potential (Ali & Coombes, 2002). We have shown (i) that a voltage-gated sodium channel (VGSC), Nav1.5, in its newly identified neonatal splice form (nNav1.5) is selectively upregulated in both the human metastatic BCa cell line MDA-MB-231 and biopsy tissues and (ii) that VGSC activity enhances metastatic cell behaviours (Fraser et al. 2005). Thus, oestrogen signalling and VGSC expression/activity could be functionally associated. Oestrogen classically works as a transcriptional regulator through α and β oestrogen receptors (ERs). We have investigated whether oestrogen signalling could affect VGSC expression/activity.

All experiments were carried out over 48-72 h on MDA-MB-231 cells transfected with ERα. The cells were cultured as described before (Fraser et al. 2005). Data are presented as mean ± SEM. Statistical significance was determined by either unpaired *t* test or chi-squared test, as appropriate.

Real-time PCR showed that treatment with the pure ER antagonist ICI-182,780 (1 μM) for 72 h significantly increased Nav1.5 mRNA levels by 211 ± 47% (n=4). Whole-cell patch clamp recordings revealed that similar treatment over >48 h increased the proportion of cells expressing functional VGSCs. Thus, the proportion of VGSC-expressing cells rose significantly from 21 to 65% (n=73; $\chi^2 = 12.3$; df = 1; $p < 0.001$). There was no change in peak current density. As regards functional consequence, a 72 h pretreatment with ICI-182,780 significantly increased the cells' transverse migration by 32 ± 13% (p = 0.01; n = 8). The latter was determined by 'transwell' assays over 7 h which would exclude any proliferative effect.

In conclusion, under the experimental conditions used, estrogen downregulated VGSC expression and functional activity. These observations were consistent with the effect on the cells' migratory potential. Thus, for the particular cell line studied, we propose the following working hypothesis:

Oestrogen → VGSC downregulation → reduced metastatic cell behaviour.

Ali S & Coombes RC (2002). *Nature Rev Cancer* **2**, 101-115.

Fraser SP, Diss JKJ, Chioni A-M, Mycielska ME, Pan H, Yamaci RF et al. (2005). *Clin Cancer Res* **11**, 5381-5389.

This study was supported by an Amber Fellowship (PCRF) to I.O.

*Where applicable, the authors confirm that the experiments described here conform with the Physiological Society ethical requirements.*

---

PC27

## Modulation of 'A'-type $K^+$ channel current and Kv 4.2 expression by soluble amyloid $\beta_{1\text{-}40}$

T. Kerrigan[1], C. Peers[2] and H.A. Pearson[1]

*[1]Institute of Membrane and Systems Biology, University of Leeds, Leeds, UK and [2]Institute for Cardiovascular Research, University of Leeds, Leeds, UK*

We have previously shown that the Alzheimer's disease related peptide amyloid beta protein (Aβ) can increase expression of the 'A'-type $K^+$ channel current in rat cerebellar granule neurones (Ramsden *et al.* 2001). This effect was a property of the soluble form of the peptide and could not be observed following Aβ aggregation. These earlier studies used a synthetic, human form of $A\beta_{1\text{-}40}$; however, the endogenous, rat Aβ differs from human by 3 amino acids. In this study we have investigated the effects of recombinant human Aβ and compared it to the effect of Aβ with a rodent sequence.

Dissociated cultures of cerebellar granule neurones were prepared from 6-8 day old rats and maintained as reported previously (Ramsden *et al.* 2001). In separate experiments, a HEK293 cell line stably overexpressing recombinant rat Kv4.2 was used. Whole-cell patch clamp measurements of $K^+$ channel currents were carried out using quasi-physiological intra- and extracellular solutions as before (Ramsden *et al.* 2001). Stock Aβ was dissolved in DMSO before dilution in culture media to a concentration of 10nM and applied to cultures for 24 hours. Statistical differences were assessed using repeated measures ANOVA with Tukey's post-hoc test or a paired Student's t test as appropriate. Human recombinant $A\beta_{1\text{-}40}$ caused a large (1.5-fold) increase in the peak $K^+$ channel current density/voltage (I-V) relationship in cerebellar granule neurones (n=17 controls, 17 Aβ-treated cells, repeated measures ANOVA, $p < 0.05$). At a test potential of +50mV, current increased from 0.77 ± 0.16 nA/pF to 1.15 ± 0.16 nA/pF. Similarly, treatment with synthetic rat $A\beta_{1\text{-}40}$ increased the I-V by 2-fold from 0.71 ± 0.14 nA/pF to 1.45 ± 0.19 nA/pF at +50mV (n=19 control, 19 Aβ-treated cells, repeated measures ANOVA, $p < 0.05$).

The inactivating, 'A'-type, component of the $K^+$ current I-V was particularly sensitive to the effects of synthetic rat $A\beta_{1\text{-}40}$ (3.4-fold increase, n=19 control, 19 treated cells, repeated measures ANOVA, $p < 0.05$) and of human recombinant $A\beta_{1\text{-}40}$ (2.6-fold increase, n=17 control, 17 treated cells, repeated measures ANOVA, $p < 0.05$).

The selective Kv 4.2 subunit blocker heteropodatoxin (75nM) was applied to investigate the effects of $A\beta_{1\text{-}40}$ on the Kv 4.2 subunit. In control experiments HEK 293 cells stably transfected with the Kv 4.2 subunit underwent substantial block of $K^+$ channel current. Mean current density at +50mV prior to application of the blocker was 1.8 ± 0.03 nA/pF whereas current after application of the blocker was 0.08 ± 0.02 nA/pF (n=3, Student's paired t test, $p < 0.05$).

These data indicate that $A\beta_{1\text{-}40}$ produced using recombinant technology has the same effect on $K^+$ channel expression as Aβ synthesised using chemical means. Furthermore, rodent and human forms of Aβ are equally effective in their ability to modulate $K^+$ channel currents.

Ramsden M, Plant LD, Webster NJ, Vaughan PFT, Henderson Z & Pearson HA (2001). *J Neurochem* **79**, 699-712.

Supported by the Alzheimer's Research Trust and MRC.

*Where applicable, the authors confirm that the experiments described here conform with the Physiological Society ethical requirements.*

---

PC28

## Inhibition of TASK3 two-pore-domain potassium channels following activation of protein kinase C

E.L. Veale, G.L. Sutton and A. Mathie

*Cell & Molecular Biology, Imperial College London, London, UK*

The TASK subfamily of two-pore-domain potassium channels (K2P) encodes for leak $K^+$ currents which contribute to the resting membrane potential of many neurons and regulate their excitability. TASK channels are highly regulated by a wide variety of pharmacological and physiological mediators. Currently, there is evidence in the literature both in favour of (Vega-Saenz de Miera *et al.* 2001) and against (Kim *et al.* 2000, Meadows & Randall, 2001) regulation of TASK3 currents by protein kinase C (PKC). We address this issue in this study.

Whole-cell electrophysiological recordings were made from tsA-201 cells, transiently transfected with wild type and mutated human (h) TASK3 channels. The phorbol ester PMA (100 nM) had no significant effect on hTASK3 mean current amplitude when applied alone (from 1715 ± 112 pA, n = 28, to 1599 ± 84 pA, n = 15, mean ± standard error, $p > 0.05$, Student's t test), but reduced mean current amplitude to 619 ± 98 pA (n = 16, $p < 0.05$) when applied together with the calcium ionophore, ionomycin (1 μM). This effect was not due to ionomycin, per se, since treatment with the inactive phorbol ester, 4αPMA and ionomycin had no effect on current amplitude (1717 ± 228 pA, n = 5, $p > 0.05$). The effect of PMA and ionomycin could be completely blocked by the non selective PKC inhibitor BIM (1 μM) (1503 ± 180 pA, n = 7) and by the 'classical' PKC inhibitor Go 6976 (100 nM) (1594 ± 144 pA, n = 8).

Selective silencing of PKCα activity with a validated siRNA sequence targeted against hPKCα caused a significant reduction in the mean current through hTASK3 channels (1181 ± 140 pA, n = 9) compared to control cells. This current was unaffected, however, following treatment with PMA and ionomycin (1310 ± 136 pA, n = 10, $p > 0.05$). In contrast, PMA and ionomycin treatment still inhibited hTASK3 current following transfection with a validated siRNA against PKCε (from 1328 ± 105 pA, n = 6 to 580 ± 128 pA, n = 8, $p < 0.05$).

The C terminus of hTASK3 contains three potential consensus sequence sites for PKC phosphorylation. Single point mutations to each of these sites in turn (S319A, S331A, T341A) were made. Whilst S319A and S331A channels were unaltered, T341A channels gave currents with a smaller amplitude than wild type and these currents were no longer inhibited by PMA and ionomycin (from 1148 ± 161 pA, n = 10 to 1050 ± 251 pA, n = 6, $p > 0.05$).

Our data show that hTASK3 channels can be strongly inhibited following activation of the classical PKC, PKCα but that the activation requires an elevation of intracellular calcium. Furthermore, PKCα produces this effect on hTASK3 by directly phosphorylating the channel at position T341 in its C terminus.

Vega-Saenz de Miera E *et al.* (2001). *J Neurophysiol* **86**, 130-142.

Kim Y *et al.* (2000). *J Biol Chem* **275**, 9340–9347.

Meadows HJ & Randall AD (2001). *Neuropharmacol* **40**, 551–559.

Supported by the MRC.

*Where applicable, the authors confirm that the experiments described here conform with the Physiological Society ethical requirements.*

---

PC29

**Is choline really a partial agonist on human muscle acetylcholine receptors?**

R. Lape, L. Sivilotti and D. Colquhoun

*Pharmacology, University College London, London, UK*

Choline is believed to be an agonist with low efficacy on muscle nicotinic acetylcholine (ACh) receptors because of a slow channel opening rate constant (Grosman & Auerbach 2000). This makes it an attractive tool in the characterization of the single channel kinetics of gain of function mutants, in which the channel opening rate constant is increased beyond its wild-type value of about 50000 $s^{-1}$ for ACh. Our mechanism-fitting analysis can resolve opening rates of up to at least 130000 $s^{-1}$ (Burzomato *et al.* 2004), but an increase in channel opening rate of more than 4-fold would be hard to measure with ACh as agonist.

We recorded choline-activated single channel currents in the cell-attached configuration from HEK293 cells transfected with human wild-type nicotinic ACh receptors (αβδε, transfection ratio 2:1:1:1).

The apparent amplitude of single channel currents decreased at high choline concentrations. This suggests that choline, like other agonists (Ogden & Colquhoun 1985) blocks the channel pore and that the blockages are too brief to be resolved as closures. The Hill slope for this effect was $n_H = 0.81 \pm 0.11$ and a fit with a Hill- Langmuir equation ($n_H = 1$) gives an estimate of the equilibrium constant for channel block as 7.6 ± 1.0 mM ($n$ = 1-3 patches per point). Openings were detected using a time-course fitting procedure (program SCAN; http://www.ucl.ac.uk/Pharmacology/dc.html). Apparent open period and shut time distributions were plotted for several choline concentrations and transmembrane potentials. At low choline concentrations (up to 1 mM), channel activations were shorter than those elicited by ACh (below 1 μM). Mean burst length: choline 0.65 ± 0.08 ms (3 patches), ACh 3.4 ± 0.3 ms (7 patches); mean apparent number of openings per burst: choline 1.11 ± 0.01, ACh 2.23 ± 0.07 ($P < 0.008$ for both by randomisation test). The distribution of apparent shut times showed an obvious fast component (Fig. 1). This fast component was not detected in studies using SKM transition detection methods (Grosman & Auerbach, 2000). Typical shut time distributions in 10 mM choline at different transmembrane potentials are shown in Fig. 1 (A: –80 mV; B: +80 mV). The time constant of the fast component did not vary with the choline concentration but was slower at positive (51 ± 16 μs; $n$ = 5 patches) than negative (13 ± 0.8 μs; $n$ = 8 patches) membrane potentials ($P = 0.0009$). Since little channel block is expected at positive potentials, the fast component may provide information about the oscillations between the open and shut states. The interpretation of the brief shut time component in terms of mechanism is still uncertain, but its observation opens the possibility that choline may have a higher efficacy than has been supposed up to now.

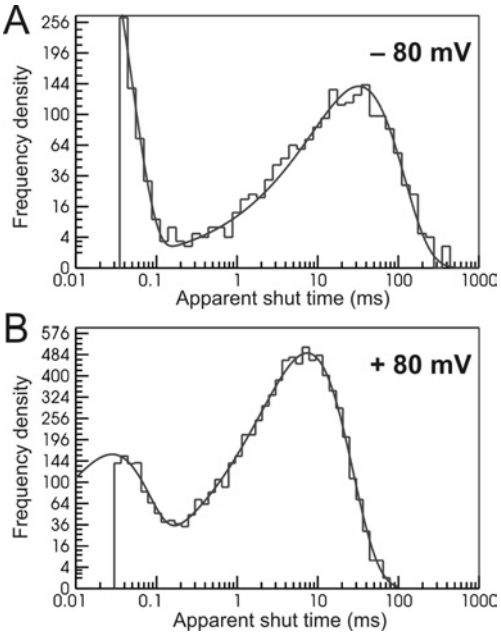


Figure 1. The distributions of apparent shut times from single channel recordings in 10 mM choline. Recording were made at two different membrane potentials, -80 mV (A) and +80 mV (B).

Burzomato V *et al.* (2004). *J Neurosci* **24**, 10924-10940.

Grosman C & Auerbach A (2000). *J Gen Physiol* **115**, 637- 651.

Ogden D & Colquhoun D (1985). *Proc R Soc Lond* **B 225**, 329-355.

This work was supported by a Wellcome Trust grant (074491).

*Where applicable, the authors confirm that the experiments described here conform with the Physiological Society ethical requirements.*

---

PC30

**Mutation of T142 located in the selectivity filter modifies gating of the inward rectifier $K^+$ channel Kir2.1**

I. Ashmole[1], P. Stansfeld[2], M.J. Sutcliffe[3] and P.R. Stanfield[1]

*[1]Dept. of Biological Sciences, The University of Warwick, Coventry, UK, [2]Department of Cell Physiology & Pharmacology, University of Leicester, Leicester, UK and [3]Manchester Interdisciplinary Biocentre, University of Manchester, Manchester, UK*

The inward rectifier $K^+$channel Kir2.1 is gated by blockage by intracellular polyamines and $Mg^{2+}$, whose occupancy of the

channel is opposed by extracellular $K^+$. An aspartate residue (D172) located in the second transmembrane domain (M2) and two glutamate residues (E224 and E299) in the cytoplasmic pore have been identified as binding sites for these blockers (for review, see Stanfield *et al.* 2002). The mechanism of channel blockage by polyamines is however not fully established. To begin to test whether polyamines come into close proximity with the channel selectivity filter, we have examined the effect of mutation of T142 in the $K^+$ selectivity sequence TIGYG on channel gating.
Channels were expressed in oocytes taken from *Xenopus* frogs. We used two-electrode voltage clamp to examine current-voltage relationships of wild type and mutant channels. Normalised conductance-voltage relationships (Fig. 1) were fitted using a Boltzmann relation with two components each of which evaluates to 0.5 at membrane potentials $V_1$ and $V_2$ with steepness factors $k_1$ and $k_2$.
$V_1$ was altered from -44.0 ± 1.0 mV (mean ± s.e.m; n = 6) in wild type to -54.4 ± 0.5 mV (n=5) in T142A, while $V_2$ = -103.9 ± 8.8 (wild type) and -115.9 ± 0.7 (T142A). $k_1$ and $k_2$ were little altered: $k_1$ = 13.7 ± 0.3 and 12.6 ± 0.4mV in wild type and T142A, respectively; $k_2$ = 20.6 ± 2.6 and 24.1 ± 0.8mV. The shift in $V_1$ to more negative values in the T142A mutant would be consistent with an increase in polyamine affinity of the mutant channels, an increase which we are in the process of testing using macropatches. Inspection of the time course of current development under hyperpolarisation is suggestive of a slower release of polyamines in the mutant.
Our results are consistent with polyamines binding deeply in the channel, in part adjacent to the intracellular end of the selectivity filter. Alternatively, since the mutation may disrupt one of the $K^+$ co-ordination sites in the selectivity filter (Zhou & MacKinnon, 2004), our results may also be explained by reduced competition between extracellular $K^+$ and the blocking polyamine. We are currently testing these hypotheses.

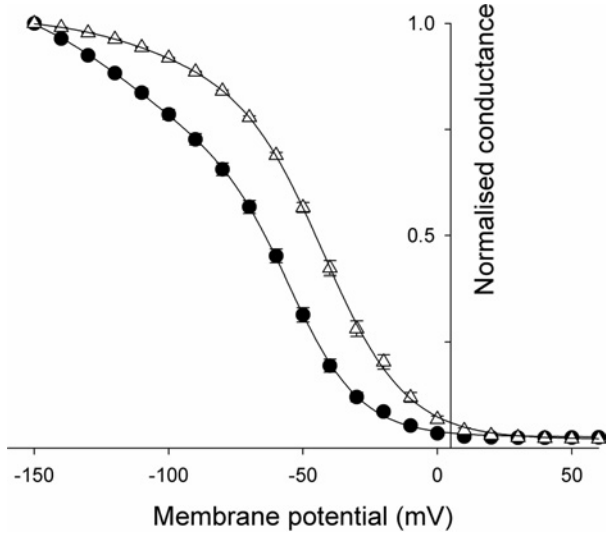


Figure 1. Relationship between normalised conductance and membrane potential for wild type Kir2.1 (open triangles) and Kir2.1 T142A (filled circles). $[K^+]_o$, 35mM.

Stanfield PR, Nakajima S & Nakajima Y (2002). Rev Physiol Biochem Pharmacol 145, 47-179.

Zhou M & MacKinnon R (2004). J Memb Biol 338, 839-846.

We thank the BBSRC for support.

*Where applicable, the authors confirm that the experiments described here conform with the Physiological Society ethical requirements.*

PC31

## Differences in the responses to metabolic poisoning between $K_{ATP}$ channel subunits

T. Farzaneh and A. Tinker

*Medicine, UCL, London, UK*

At the molecular level, $K_{ATP}$ is an octameric protein complex, composed of an inwardly rectifying $K^+$ channel subunit (Kir6.0) which forms the channel pore and a regulatory sulphonylurea receptor subunit (SUR). By sensing intracellular nucleotide concentrations, $K_{ATP}$ channels couple the membrane potassium conductance of a cell to its metabolic state.
To understand the molecular basis of metabolic regulation of the $K_{NDP}/K_{ATP}$ channels Kir6.1/SUR2B and Kir6.2/SUR2A, the cell-based Rubidium-86 ($^{86}Rb^+$) efflux assay was employed, using HEK293 cells as the expression system. After channel activation the $^{86}Rb^+$ distribution between intracellular and extracellular space was determined via the measurement of Cherenkov radiation, the relative amount of $^{86}Rb^+$ in the cell supernatant being a direct measure of channel activity. $^{86}Rb^+$ efflux was activated on the addition of 10μM levcromakilim, 10μM diazoxide and metabolic poisoning (induced by 20mM 2-deoxyglucose and 2.5mM sodium cyanide), and inhibited by 10μM glibenclamide. Co-expression of SUR and Kir6.0 is necessary to shield their respective RKR retention motifs, generate plasmalemmal currents and allow cell surface expression of the channel. Kir6.2ΔC26 has previously been shown to form ATP-sensitive channels in the absence of SUR1 (1), and deletion of the N-terminus of Kir6.0 has been found to increase basal activity (2). Kir6.1 C-and N-terminal truncations were made to delete the RKR motif, enabling understanding of the role of each subunit pharmacologically in channel gating. Immunofluorescent staining using an anti-HA-fluorescein conjugated antibody confirmed that removal of the RKR motif allows surface expression.
Kir6.1/SUR2B and Kir6.2/SUR2A were initially characterised to determine the time at which the linear phase of efflux was achieved after incubation with agonist, upon which Kir6.1ΔN and ΔC were screened to determine functionality. Kir6.1Δ48C/ΔN13 was found to be constitutively active without SUR2B. When expressed with SUR2B glibenclamide was able to reverse metabolic inhibition, suggesting that the SUR was responsible for channel regulation under this condition. However, when mutations were introduced into nucleotide binding domain 1 (NBD) or NBD2 (K708A and K1349M respectively) of SUR2B and expressed with Kir6.1, normal pharmacology was observed, suggesting that neither NBD is independently involved in metabolic regulation.
Metabolic inhibition was induced when Kir6.2ΔC26 was expressed without the SUR subunit, which was reversed via $BaCl_2$ (a pore blocker). Since Kir6.1Δ48C was not found to be metabolically sensitive when expressed alone, this further suggests that Kir6.1 is not involved in metabolic regulation, but that Kir6.2 is. Overall, this highlights a difference in metabolic regulation between Kir6.1 and Kir6.2 forming channels.

Reimann F, Tucker SJ, Procks P & Ashcroft FM (1999). *J Physiol* **518**, 325-336.

Babenko AP & Bryan J (2001). *J Biol Chem* **276**, 49083-49092.

*Where applicable, the authors confirm that the experiments described here conform with the Physiological Society ethical requirements.*

PC32

**Splice variants of human Nav1.5 voltage-gated $Na^+$ channel: an electrophysiological comparison**

J. Mattis[2], R. Onkal[3], S.P. Fraser[1], J.K. Diss[4] and M.B. Djamgoz[1]

*[1]Division of Cell and Molecular Biology, Imperial College London, London, UK, [2]Department of Molecular Cellular and Developmental Biology, Yale University, New Haven, CT, USA, [3]Department of Neuroscience and Maths, Macalester College, St Paul, MN, USA and [4]Medical Molecular Biology Unit, Institute of Child Health, London, UK*

We recently identified a 'neonatal' splice variant of Nav1.5 (nNav1.5) in metastatic human breast cancer (BCa) cells (Fraser et al. 2005). The splicing results from the alternate inclusion of two exons (the 5' genomic and the 3' genomic) encoding D1:S3 and the D1:S3/S4 extracellular linker of the voltage-gated $Na^+$ channel (VGSC). The 'neonatal' (5' exon) splice variant has 31 nucleotide differences from the 'adult' (3' exon) form (aNav1.5) that results in 7 amino acid substitutions. Of particular note is the replacement of the 3' exon aspartate with a positively charged lysine residue (Chioni et al. 2005). The aim of the present study was to investigate the possible electrophysiological consequences of the Nav1.5 D1:S3 splicing. All data are presented as mean ± standard errors of the mean. Statistical significance was determined by unpaired *t* test (n>16 cells for each test).

Whole-cell patch clamp recording from transfected EBNA-293 cell lines (Chioni et al. 2005) revealed that aNav1.5 and nNav1.5 activated at -59.7 ± 0.8 mV and -57.8 ± 0.9 mV (P = 0.12) and peaked at -20.3 ± 1.0 mV and -14.2 ± 2.1 (P < 0.01), respectively. The normalized conductance-voltage relationship fitted to a Boltzmann distribution indicated half-activation voltages of -40.6 ± 0.2 mV and -33.8 ± 0.2 mV for aNav1.5 and nNav1.5 (P < 0.001) whilst the slope factors were 6.2 ± 0.2 mV and 7.1 ± 0.2 mV(P < 0.01), respectively. In addition, the half-inactivation voltages for aNav1.5 and nNav1.5 were -94.5 ± 0.4 and -96.0 ± 0.4 mV (P < 0.01), whilst the slope factors were -6.8 ± 0.4 mV and -7.3 ± 0.3 mV (P = 0.43), respectively. The 'adult' and 'neonatal' Nav1.5 VGSCs differed notably in their kinetics of activation and inactivation. For both splice variants, time to peak decreased with increasing depolarization, from 1.41 ± 0.06 ms at -40 mV to 0.67 ± 0.02 ms at 0 mV (for aNav1.5) and from 1.82 ± 0.07 ms at -40 mV to 0.78 ± 0.03 ms at 0 mV (for nNav1.5). Over the voltage range -30 mV to 0 mV, nNav1.5 activated significantly more slowly than the 'adult'. The fast and slow inactivation time constants were significantly smaller for aNav1.5 vs nNav1.5 for most voltages analyzed. On the other hand, the time courses of recovery from inactivation were the same at given voltages.

In conclusion, significant differences were found in the electrophysiological characteristics of the 'adult' and 'neonatal' splice variants of Nav1.5 *in vitro*. Further understanding of such properties *in vivo* would be of importance for developmental physiology and clinical management of BCa (Fraser et al. 2005).

Chioni A-M, Fraser SP, Pani F, Foran P, Wilkin GP, Diss JKJ & Djamgoz MBA (2005). *J Neurosci Methods* **147**, 88-98.

Fraser SP, Diss JKJ, Chioni A-M, Mycielska ME, Pan H, Yamaci RF et al. (2005). *Clinical Cancer Research* **11**, 5381-5389.

This study was supported by the Pro Cancer Research Fund (PCRF).

*Where applicable, the authors confirm that the experiments described here conform with the Physiological Society ethical requirements.*

PC33

**Inhibitory gating modulation of small conductance calcium-activated potassium channels by NS8593 reduces the SK-mediated afterhyperpolarising current in hippocampal CA1 neurones**

R.D. Taylor[1], D. Strøbæk[2], C. Hougaard[2], T.H. Johansen[2], U.S. Sørensen[2], E.Ø. Nielsen[2], K.S. Nielsen[2], P. Pedarzani[1] and P. Christophersen[2]

*[1]Dept of Physiology, University College London, London, UK and [2]NeuroSearch A/S, Ballerup, Denmark*

SK channels are small conductance $Ca^{2+}$-activated $K^+$ channels important for the control of neuronal excitability and fine tuning of firing patterns and synaptic function (Stocker, 2004). The classical SK channel pharmacology has largely focused on the peptide apamin, which acts extracellularly by a pore blocking mechanism (Strong, 1990; Ishii et al. 1997). Recently, 1-EBIO (Pedarzani et al. 2001) and NS309 (Pedarzani et al. 2005) have been identified as SK channel enhancers or positive gating modulators, which work by increasing the apparent $Ca^{2+}$ sensitivity of SK channels. Here we describe negative gating modulation as a novel principle for selective inhibition of SK channels. In whole-cell patch clamp experiments the benzimidazol-based compound NS8593 reversibly inhibited recombinant rat SK3-mediated currents with a $K_i$ value of 90 ± 8 nM (n=33). However, in contrast to known pore blockers, NS8593 did not inhibit [$^{125}$I]apamin binding in assays performed on HEK293 cells expressing human (h) SK3 channels or rat striatal membranes. Using excised patches, it was demonstrated that NS8593 decreased the apparent $Ca^{2+}$ sensitivity of hSK channels by shifting to the right the activation curve for $Ca^{2+}$, without affecting the maximal $Ca^{2+}$-activated SK current. In the absence of NS8593, hSK3 channels were highly sensitive to $Ca^{2+}$ with an $EC_{50}$ of 0.43 μM and a Hill coefficient of 5.5 (n=17). In the presence of 3 μM NS8593, the channels had a reduced $Ca^{2+}$ sensitivity with an $EC_{50}$ of 2 μM and a Hill coefficient of 2.8 (n=3). The shift in the $Ca^{2+}$ activation curve indicated that the effect of NS8593 was pronounced at low $Ca^{2+}$ concentrations, whereas the inhibition of hSK3 currents by NS8593 was fully abolished at 100 μM $Ca^{2+}$. Similar $Ca^{2+}$ activation curves were obtained for hSK1- and hSK2-mediated currents, showing that the affinity for NS8593 was $Ca^{2+}$-dependent on these SK channel subtypes. The potency of NS8593 was similar at hSK1, hSK2, and hSK3 channels, but the compound did not affect hIK or hBK channels. The site of action of NS8593 was accessible from both sides of the membrane and the

inhibition was prevented in the presence of high concentrations of the positive modulator NS309. NS8593 was further tested in whole-cell patch clamp experiments on mouse CA1 neurons in hippocampal slices. NS8593 strongly inhibited (84.7±1.4% inhibition at 3 μM, n=3; 86.7 ± 5.1% inhibition at 10 μM, n=6) the apamin- and tubocurarine-sensitive SK-mediated afterhyperpolarising current $I_{AHP}$ elicited by 100 ms long depolarising pulses (as in Pedarzani et al. 2005).

Ishii TM, Maylie J & Adelman JP (1997). J Biol Chem 272, 23195-23200.

Pedarzani P, Mosbacher J, Rivard A, Cingolani LA, Oliver D, Stocker M, Adelman JP & Fakler B (2001). J Biol Chem 276, 9762-9769.

Pedarzani P, McCutcheon JE, Rogge G, Jensen BS, Christophersen P, Hougaard C, Strøbæk D & Stocker M (2005). J Biol Chem 280, 41404-41411.

Stocker M (2004). Nat Rev Neurosci 5, 758-770.

Strong PN (1990). Pharmacol Ther 46, 137-162.

We thank Dr M. Stocker for useful discussion; H. D. Rasmussen and T. Sparre for assistance with the synthesis of NS8593; J. Sonne, A. S. Meincke and V. Meyland-Smith for help with patch clamp experiments. This work was supported by the MRC.

*Where applicable, the authors confirm that the experiments described here conform with the Physiological Society ethical requirements.*

---

PC34

## Endocytic trafficking of the hERG potassium channel

D. Elliott, T. Taneja, A. Smith, K. Aviss and A. Sivaprasadarao

*University of Leeds, Leeds, UK*

The hERG potassium channel is a voltage-gated potassium ($K_v$) channel, which plays a key role in the repolarisation of the cardiac action potential. Genetic mutations in the hERG channel have been shown to cause long QT syndrome type 2 (LQT2) by several mechanisms; some alter the functional properties of the channel while others impair the trafficking of newly synthesised hERG protein from the ER to the membrane (1).

The density of cell surface receptors and channels is regulated not only by the biosynthetic pathways, but also via endocytic mechanisms and these processes play an important role in cell physiology (2). The fate of the hERG channel subsequent to membrane insertion is, however, currently unknown. Here we investigated whether the hERG potassium channel undergoes endocytosis and recycling.

hERG channels containing a HA (haemagglutinin A) epitope introduced into an extracellular loop were expressed either transiently or stably in HEK 293 cells. The cell surface channels were first bound with anti-HA antibody at 4°C and their trafficking was followed at 37°C using standard immunocytochemistry and confocal microscopy.

Results show that internalisation of hERG channels occurred within 30 min of incubation at 37°C. Internalisation could be prevented by either $K^+$ depletion or hypertonicity (induced with 0.45 M sucrose). Both $K^+$ depletion and hypertonicity are known to specifically prevent clathrin-mediated endocytosis. Internalisation of Alexafluor488-conjugated transferrin was also prevented under these conditions indicating that the hERG channel undergoes endocytosis via clatharin-coated vesicles.

We next examined if the internalised hERG channels were able to recycle back to the plasma membrane. For this we allowed the HA antibody labelled channels to internalise for 2 hrs; cells were then stripped of remaining surface antibody and kept at 37°C to follow recycling. The results showed that the labelled channels returned to the cell surface within 15 min. This recycling could be prevented by pre-treatment of cells with 60 μM primaquine, a known blocker of protein recycling. These data suggest that the internalised hERG channels are able to recycle back to the plasma membrane.

To investigate the route of endocytic trafficking, we have co-transfected the hERG channel with GFP-conjugated markers for various endocytic compartments. Co-localisation was observed with markers of early and sorting endosomes and the endocytic recycling compartments. Co-localisation was also observed with late endosomal and lysosomal markers. These data suggest that while some of the internalised channels are able to recycle, others may undergo lysosomal degradation.

In conclusion, our data provide evidence for endocytosis and recycling of the hERG channel. The physiological importance of endocytic trafficking of hERG has yet to be elucidated.

Anderson CL, Delisle BP, Anson BD, Kilby JA, Will ML, Tester DJ et al. (2006). Circulation 113, 365-373.

Maxfield FR & McGraw TE (2004). Nat Rev Mol Cell Biol 5, 121-132.

This work was supported by the British Heart Foundation.

*Where applicable, the authors confirm that the experiments described here conform with the Physiological Society ethical requirements.*

---

PC35

## Barium block of inward rectifier potassium channels: comparison of cultured human pulmonary smooth muscle cells with cloned Kir2.1 and 2.4

B.P. Tennant, Y. Cui, A. Tinker and L.H. Clapp

*Medicine, University College London, London, UK*

Strong inward rectifier $K^+$ currents ($K_{IR}$), carried by Kir2.0 channels, are thought to contribute to the resting membrane potential in smooth muscle, predominantly through Kir2.1 (1). Kir2.0 currents differ in their sensitivity to barium inhibition and all, except Kir2.4, show a characteristic voltage and time-dependence to the block (2).

We electrophysiologically characterised the $Ba^{2+}$ inhibition of $K_{IR}$ currents, comparing native human pulmonary arterial smooth muscle (HPASM) cell currents with cloned Kir2.1 or Kir2.4.

Whole-cell currents were recorded from HPASM cells and HEK293 cells, stably transfected with Kir2.1 or Kir2.4, in the presence of a 60/140mM $K^+$ gradient. At a holding potential of -20mV, voltage steps were applied from -150mV to +20mV and extracellular $Ba^{2+}$ block of current was examined (0.1μM-10mM). The concentration dependency of barium block was assessed through inhibition curves at various membrane potentials (Table 1a). Interestingly, the Hill coefficient for $K_{IR}$ in HPASM cells was shallow (~0.4), which may represent a contribution from at least two distinct molecular components to the current. Kir2.1 currents showed greater sensitivity to $Ba^{2+}$ com-

pared with those of Kir2.4 and HPASM cells at -120mV. Currents from all three cells showed distinct $Ba^{2+}$ sensitivities at -80mV, with HPASM cells being intermediate. Kir2.1, additionally showed a 2-fold decrease in $Ba^{2+}$ sensitivity when depolarised from -120 to -80mV ($p<0.01$) whereas Kir2.4 and HPASM cells showed no significant decrease (t test).

The voltage dependence of $Ba^{2+}$ block of $K_{IR}$ was assessed quantitatively using the approach of Woodhull (3), the parameters of which are shown in Table 1(b).The fractional distance of $Ba^{2+}$ block into the transmembrane field, $\delta$, for Kir2.1 was distinct from that of Kir2.4 and $K_{IR}$ in HPASM cells, which themselves were indistinct. The $K_D(0)$ value reflects the sensitivity to $Ba^{2+}$ block at 0mV and thus removes any contribution of voltage dependence. Currents in HPASM cells were different to both Kir2.1 and Kir2.4 currents, but Kir2.1 and Kir2.4 were not distinct.

Together these data suggest that the molecular components of $K_{IR}$ currents in HPASM cells are not solely composed of Kir2.1. The characteristics described here, indicate that more than one Kir2.0 channel may contribute and that $Ba^{2+}$ block of HPASM cell $K_{IR}$ shares more similarity to Kir2.4 than Kir2.1.

| | (a) $Ba^{2+}$ $K_D$(Vm) (μM) | | (b) [$Ba^{2+}$] 100 μM | |
|---|---|---|---|---|
| $K_{IR}$ | Vm = -120mV | Vm = -80mV | $K_D(0)$ (μM) | δ |
| Kir2.1 n=10 | 3.1 ± 0.4 (Hill 0.91±0.11) | 6.1 ± 0.8 (Hill 0.80±0.08) | 142.1 ± 23.2 | -0.77 ± 0.08 |
| Kir2.4 n=9 | 60.1 ± 9.2*** (Hill 0.78±0.08) | 78.1 ± 13.3*** (Hill 0.87±0.12) | 197.1 ± 17.7 | -0.30 ± 0.03 *** |
| HPASM n=9 | 45.2 ± 14.8**/ns (Hill 0.36±0.05) | 49.4 ± 8.8**/# (Hill 0.35±0.02) | 337.1 ± 44.8 ***/## | -0.43 ± 0.05 ***/ns |
| One way ANOVA: p-value vs Kir2.1 **<0.01,***<0.001; Kir2.4 #<0.05, ##<0.01 | | | | |

Table 1

Bradley KK *et al.* (1999). *J Physiol* **515**, 639-651.

Stanfield PR *et al.* (2002). *Rev Physiol Biochem Pharmacol* **145**, 47-179.

Woodhull AM (1973). *J Gen Physiol* **61**, 687-708.

This work was funded by The British Heart Foundation.

*Where applicable, the authors confirm that the experiments described here conform with the Physiological Society ethical requirements.*

## PC36

### Lysosomal targeting of P2X4 receptors and protection from degradation by N-linked glycosylation

A. Paramasivam, O.S. Qureshi and R.D. Murrell-Lagnado

*Department of Pharmacology, University of Cambridge, Cambridge, UK*

P2X4 receptors are a subtype of ATP-gated cation channel and are composed of two transmembrane domains, an extracellular ligand binding site and intracellular N- and C-termini. Peripheral nerve damage has been demonstrated to cause upregulation of the receptor resulting in tactile allodynia, which was reduced following adminstration of P2X4 anti-sense oligodeoxynucleotides (Tsuda et al. 2003). When heterologously expressed in neurones and human embryonic kidney (HEK-293) cells P2X4 receptors undergo constitutive endocytosis through an interaction with a non-canonical tyrosine based motif and adaptor protein-2 (Bobanovic et al. 2002; Royle et al. 2002; Royle et al. 2005). Recent work in primary macrophages has shown that P2X4 receptors are predominantly located within lysosomes, where they retain their function and can be delivered to phagosomes and the plasma membrane (unpublished observations, Qureshi & Murrell-Lagnado). We show by immunocytochemistry in normal rat kidney (NRK) cells that targeting of rat P2X4 receptor to lysosomes involves a dileucine type motif in the N-terminus in addition to previously identified tyrosine based motifs in the C-terminus (Royle et al. 2002). Mutation of these motifs results in increased surface expression of the receptor. When both the tyrosine and dileucine motifs are mutated there is reduced lysosomal localisation of the receptor. Furthermore, Western blot analysis demonstrates that the P2X4 receptor remains stable within the proteolytic environment of the lysosomes. Seven potential N-linked glycosylation sites have been identified on the extracellular loop of P2X4 and we provide evidence that at least six are glycosylated. Removal of these glycans in vivo with endoglycosidase H results in the rapid degradation of the receptor. Our results show that P2X4 receptors are targeted to lysosomes by dileucine- and tyrosine-based motifs, where they are protected from degradation by N-linked glycosylation.

Tsuda M, Shigemoto-Mogami Y, Koizumi S, Mizokoshi A, Kohsaka S, Salter MW & Inoue K (2003). Nature 424, 778-783.

Bobanovic LK, Royle SJ & Murrell-Lagnado RD (2002). J Neurosci 22, 4814-4824.

Royle SJ, Bobanovic LK & Murrell-Lagnado RD (2002). J Biol Chem 277, 35378-35385.

Royle SJ, Qureshi OS, Bobanovic LK, Evans PR, Owen DJ & Murrell-Lagnado RD (2005). J cell Sci 118, 3073-3080.

This work was supported by the Biotechnology and Biological Sciences Research Council.

*Where applicable, the authors confirm that the experiments described here conform with the Physiological Society ethical requirements.*

## PC37

### Pharmacological dissection and distribution patterns of NaN/Nav1.9, T-type $Ca^{2+}$ currents and mechanically activated cation currents in different subpopulations of rat nociceptors

B. Coste, M. Crest and P. Delmas

*LNPC UMR6150, CNRS, Marseille, France*

Dorsal root ganglion (DRG) neurones express a unique repertoire of ion channels, including the tetrodotoxin-resistant (TTX-R) low-threshold $Na^+$ channel Nav1.9/NaN and the low-threshold T-type $Ca^{2+}$ channel(s). These channels have been shown to be implicated in the molecular mechanisms of pain transmission.

As part of ongoing work aimed at illuminating the functional role of Nav1.9 and T-type $Ca^{2+}$ channels (ICaT) in sensory neurones, we have used whole-cell patch clamp recording combined with pharmacological methods to determine the relative contribution of Nav1.9 and ICaT to low-threshold (LVA) currents in acutely dissociated rat DRG neurons. We showed that amiloride blocked ICaT whereas it had no effects on Nav1.9 as well as Nav1.8/SNS currents. We next sought to characterize NaN/Nav1.9 currents pharmacologically using amiloride as a discriminating tool. Nav1.9/NaN was inhibited by various inorganic $Ca^{2+}$ channel blockers with the following rank of potency (IC50, μM): $La^{3+}$ (46) > $Cd^{2+}$ (234) > $Ni^{2+}$ (893). We then devised a classification system based on several characteristics, including cell body diameter, capsaicin sensitivity and the presence and properties of NaN/Nav1.9, ICaT and mechanosensitive cation currents. Cluster analysis identified 2 subpopulations among the C-heat nociceptive cells (Cm from 14-40 pF, n = 68). These 2 groups had identical Nav1.9 current density but significantly different densities of amiloride-sensitive ICaT (group-I: 6.5 ± 1 pA/pF; group-II: 35 ± 5 pA/pF). In addition, group-II C-heat nociceptive cells exhibited an amiloride-resistant ICaT (5.5 ± 2 pA/pF). Cells clustered in group-I displayed high-threshold slowly-adapting mechanically-activated currents whereas group-II cells had mechanically-activated currents which failed to adapt during the entire length of mechanical stimuli. We identified a third population of nociceptive cells that made up ~35 % of the capsaicin-responsive cell population, and which fell mainly within the medium cell range (Cm = 35-70 pF, n = 37), possibly corresponding to type Aδ DRG cells. This cell subset was not mechanosensitive and had very large NaN/Nav1.9 current (37.2 ± 3 pA/pF) and relatively small amiloride-sensitive ICaT (18.5 ± 4 pA/pF). In conclusion, this study shows that Nav1.9 and T-type $Ca^{2+}$ currents are co-expressed in C-type and Aδ nociceptors and cannot be distinguished by their sensitivity to inorganic $Ca^{2+}$ channels. In addition, the use of amiloride as a discriminating tool allowed us to identify 2 subpopulations of C-type nociceptors that may be distinguished by their relative expression of NaN/Nav1.9, T-type $Ca^{2+}$ currents and mechanosensitive cation currents. Results are presented as mean ± SEM.

This work is supported by the CNRS and by grants from the Agence Nationale de la Recherche.

*Where applicable, the authors confirm that the experiments described here conform with the Physiological Society ethical requirements.*

---

PC38

## Modulatory role of post-synaptic density 95 (PSD-95) and insulin receptor kinase on Kv1.3 biophysics and trafficking

D.R. Marks[1] and D.A. Fadool[1]

*[1]Program in Neuroscience, Florida State University, Tallahassee, FL, USA and [2]Molecular Biophysics, Florida State University, Tallahassee, FL, USA*

Previous work by our laboratory has demonstrated a pivotal role for the voltage-gated *Shaker* potassium channel (Kv1.3), highly expressed in the olfactory bulb (OB), in acuity, threshold, and odorant discrimination (Fadool *et al.* 2004). The insulin receptor (IR) kinase is expressed at high levels in the mouse OB where it is found to suppress 36 ± 4% of Kv1.3 current via tyrosine phosphorylation of critical N and C terminal residues (Fadool *et al.* 1998). We now show using patch-clamp electrophysiology that the adaptor protein post-synaptic density 95 (PSD-95) disrupts insulin-evoked Kv1.3 current suppression and restores peak current amplitude to 98 ± 5% of initial peak current. PSD-95 also exhibits strong modulatory effects alone on mouse Kv1.3 channel inactivation kinetics by speeding the channel inactivation by 52 ± 4%. We used immunocytochemistry and confocal microscopy to show that all three proteins are co-localized in the mouse OB, with PSD-95 showing heavy labelling across all neurolamina including the glomeruli. Using SDS-PAGE and Western blot we found that PSD-95 co-immunoprecipitates with Kv1.3, as well as the IR kinase, demonstrating a multiple protein-protein interaction in the heterologous expression system of human embryonic kidney (HEK293) cells. Confocal imaging revealed PSD-95 clusters Kv1.3 in transfected HEK293 cell membranes, as well as clusters the IR kinase, but only in the presence of Kv1.3. A PSD-95 mutant lacking the $SH_3$ and guanylate kinase (GK) domain (PSD-95 ΔSH3) was constructed by cDNA truncation of PSD-95, as well as use of previous mutants created by El-Husseini *et al.* (2000) to dissect the interaction of these three proteins through co-immunoprecipitation and confocal microscopy. The PSD-95 ΔSH3 mutant fails to cluster the IR kinase with Kv1.3 in HEK293 cell membranes, suggesting the IR kinase-PSD-95 protein-protein interaction is mediated by the PSD-95 $SH_3$ domain. PSD-95 ΔPM (minus palmitoylation mutant) was also used to demonstrate that PSD-95 may be involved in the trafficking and distribution of Kv1.3 by visualizing channel membrane and cytosol distribution in transfected HEK293 cells using confocal microscopy. We propose a model of interaction of Kv1.3, IR kinase, and PSD-95 where Kv1.3 channels are bound by PDZ domains 1 and 2 of PSD-95 and the IR kinase is bound by the $SH_3$ domain. These data suggest that PSD-95 may influence the excitability of synaptic connections in the mouse OB via K channel interaction and subsequent modulation.

El-Husseini AE, Craven SE, Chetkovich DM, Firestein BL, Schnell E, Aoki C & Bredt DS (2000). J Cell Biol 148, 159-172.

Fadool DA & Levitan IB (1998). J Neurosci 18, 6126-6137.

Fadool DA, Tucker K, Perkins R, Fasciani G, Thompson RN, Parsons AD et al. (2004). Neuron 41, 389-404.

Supported by the National Institutes of Health (NIH DC03387; NIDCD) and the FSU Council on Graduate Studies (COG).

*Where applicable, the authors confirm that the experiments described here conform with the Physiological Society ethical requirements.*

---

PC39

## Gain-of-function in Kir2.1 and its effects on atrial fibrillation in homogeneous virtual human atrial tissue: a computer simulation study

S. Kharche[1], H. Moore[1], C. Garratt[2], J. Hancox[3] and H. Zhang[1]

*[1]School of Physics and Astronomy, University of Manchester, Manchester, Lancashire, UK, [2]Manchester Royal Infirmary, University of Manchester, Manchester, Lancashire, UK and [3]Department of Physiology, University of Bristol, Bristol, Gloucestershire, UK*

Familial atrial fibrillation (AF) has been causatively linked to Kir2.1 V93I gene mutation, which manifests as gain-of-function

in IK1 [1]. In this study we evaluated the role of this gene mutation in initiation and maintenance of AF in humans.

Experimental data of voltage-dependent increase in IK1 due to Kir2.1 V93I mutation [1] was incorporated into the Courtemanche *et al.* model of electrical action potential (AP) of human atrial cell for wild (WT), heterozygous (HMT) and mutant conditions (MT). Single cell restitutions in AP and effective refractory period (ERP) were computed using a standard S1-S2 protocol [2]. The single cell model was then incorporated into a partial differential equation to simulate homogeneous 1D and 2D tissues. S1-S2 protocols were used to compute restitution in conduction velocity (CV). In 2D tissue, re-entry was initiated using a cross-field protocol and dynamics characterized using life span (LS), tip meandering and number of wavelets during a 10 s simulation.

Increased IK1 abbreviated atrial AP (Fig. 1) and flattened APD (Fig. 2), ERP, and CV restitution curves. It hyperpolarized atrial resting potential and reduced atrial excitability, which resulted in reduction of intra-atrial CV. In the 2D model re-entry self-terminated for WT (LS ~ 3s) and HWT (LS ~ 1.8s) tissues, but persisted in MT (LS >10 s). In all 3 tissue types, re-entry was unstable with breakup and formation of multiple wavelets. Within the same atrial mass (37.5 x 37.5 $mm^2$), the WT and HWT tissues accommodated a maximum of only 3 wavelets, the WT tissue accommodated 7. Tip meander of re-entry was over a larger area in WT and HT tissues than in MT.

Gain-of-function of IK1 shortens atrial APD and ERP facilitating re-entrant circuits. It increases LS of re-entrant waves while reducing the meander, thus increasing stability. This study contributes towards understanding how Kir2.1 V93I mutation facilitates and perpetuates AF in humans.

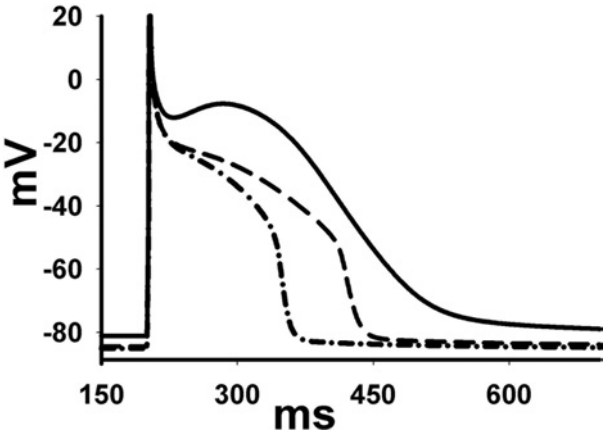


Figure 1. Changes in APD due to gain-of-function in IK1. WT AP profile is shown as solid line (APD = 322.73 ms), HMT as dashed line (APD = 257.7 ms), and the MT as dashed-dotted line (APD = 225.68 ms). The APD decreased by 20.67 % in HMT case, and by 30.24 % in the MT case. Changes in APD associated with gain-of-function in IK1 are not available.

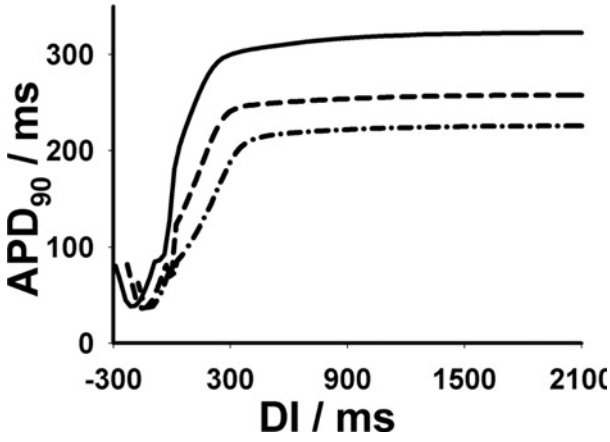


Figure 2. Changes in cell AP restitution due to gain-of-function in IK1. WT restitution is shown as solid line (maximal slope = 2.3), HMT as dashed line (maximal slope = 2.2261), and MT as dashed-dotted line (maximal slope = 0.4608). Changes in restitution associated with gain-of-function in IK1 are not available.

Xia *et al.* (2005) *Biochem Biophys Res Comm* **332**, 1012-1019.

Workman *et al.* (2001). *Cardiovas Res* **52**, 226-235.

This work was supported by a BHF grant PG/03/140.

*Where applicable, the authors confirm that the experiments described here conform with the Physiological Society ethical requirements.*

---

PC40

**Protection of Swiss-Webster mouse cerebellar granule neurons by potassium channel blockers**

A. Collins, M.K. Larson, J.E. Pfaff and J.E. Ishmael

*Pharmaceutical Sciences, Oregon State University, Corvallis, OR, USA*

Mechanisms of neuronal survival and degeneration are central to the understanding of neurodegenerative diseases. Cerebellar granule neurons (CGN) have been widely used as a model system for studying these mechanisms. It is well known that the survival of rat CGN in culture is promoted by supra physiological extracellular potassium ion concentrations ($[K^+]_o$), but whether mouse CGN have a similar requirement for elevated $[K^+]_o$ may depend upon the mouse strain [1]. To add to this body of knowledge, we tested the effect of $[K^+]_o$ on the survival of CGN from Swiss-Webster mice, a common laboratory strain. CGN were prepared from cerebella of 4-5 day old mouse pups and cultured for 5 days in Modified Eagle's Medium (MEM) with 25 mM $[K^+]$ and fetal bovine serum. The medium was then changed to serum-free MEM with 5.6 mM $[K^+]$, or 25 mM $[K^+]$ as control. Cell viability was assayed 24 hours later by 3-(4, 5-dimethylthiazolyl-2)-2, 5-diphenyltetrazolium bromide reduction (MTT assay), and was 48 ±1.3% (mean±sem) in 5.6 mM $[K^+]_o$ compared to 25 mM $[K^+]_o$ (1.7% sem; $p<0.0001$, t test). CGN and other cell types have been reported to be protected by potassium channel blockers, with different blockers being effective in different cell types. We tested the protective effects of potassium channel blockers on Swiss-Webster CGN and found a limited degree of protection in 5.6 mM $[K^+]_o$ by 2 mM 4-aminopyridine (4-AP; 63±2.2%; $p<0.001$), 2 mM tetraethylammonium (TEA; 58±1.7%;

p<0.01) and 1 mM $Ba^{2+}$ (66±1.3%; p<0.001) by ANOVA vs 5.6 mM $[K^+]_o$ alone (47±1.0%). The protective effect of these blockers was additive; survival in 5.6 mM $[K^+]_o$ plus 4-AP, TEA and $Ba^{2+}$ (98±2.2%) was equivalent to survival in 25 mM $[K^+]_o$ without blockers (1.4% sem). The neuroprotective effect of elevated $[K^+]_o$ is reported to be attenuated by L-type $Ca^{2+}$ channel blockers in rat CGN [2,3]. We found a similar effect of 2 μM nifedipine on Swiss-Webster CGN (78 ±1.8% survival); p<0.001 by ANOVA vs 25 mM $[K^+]_o$ (3.4% sem), but nifedipine did not attenuate the neuroprotective effect of potassium channel blockers (p>0.05 by ANOVA). Taken together, these results suggest that the survival of CGN depends on the total potassium permeability of the membrane rather than the activity of a particular type of potassium channel, and that the mechanism of neuroprotection by potassium channel blockers does not involve voltage-dependent influx of $Ca^{2+}$. (Note: For results reported here, n≥18 from at least two separate experiments.)

Fujikawa N et al. (2000). Eur J Neurosci 12, 1838-1842.

Gallo V et al. (1987). J Neurosci 7, 2203-2213.

Galli C et al. (1995). J Neurosci 15, 1172-1179.

Funded by Oregon State University Research Office and Department of Pharmaceutical Sciences.

*Where applicable, the authors confirm that the experiments described here conform with the Physiological Society ethical requirements.*

---

PC41

**CFTR: an ABC transporter turned channel**

P. Vergani[1], S. Lockless[2], C. Basso[2], A.C. Nairn[2] and D.C. Gadsby[2]

*[1]Pharmacology, University College London, London, UK and [2]The Rockefeller University, New York, NY, USA*

CFTR, whose dysfunction causes the disease cystic fibrosis, belongs to the ubiquitous superfamily of ABC proteins, which bind and hydrolyze ATP at conserved nucleotide-binding domains (NBDs). Most ABC proteins comprise membrane-spanning domains and couple ATP hydrolysis to translocation of solutes. CFTR is unique in that its transmembrane domains comprise a $Cl^-$ channel, and ATP binding and hydrolysis at its NBDs control opening and closing of the ion-permeation pathway. Since it is likely that ABC proteins might share a common conformational coupling mechanism, linking hydrolytic cycle to conformational changes in the TMDs, we have investigated CFTR's gating mechanism starting from the evolutionary record. In alignments of NBD sequences one can discern pairs of positions at which amino acid distribution varies in a concerted way. This correlation in evolutionary space probably reflects conservation of pairs of energetically coupled residues that mediate transmission of allosteric signals in individual ABC proteins. We selected two co-evolving positions as targets for mutagenesis, one in CFTR's N-terminal NBD1 and the other in its C-terminal NBD2. Using several single channel kinetic parameters to characterize wild-type, each of the two single mutants, and the double mutant, we could follow how the energetic coupling between the two target positions changes during CFTR's gating cycle. We found that the coupling energy obtained from thermodynamic mutant cycle analysis of ATP dependence of gating was not significantly different from zero, while mutation-linked changes in opening rate and open probability were less than additive, yielding coupling energies of –2.7±0.5 kT and –2.4±1.0 kT, respectively. These results are consistent with a scheme in which the two side-chains are not interacting in the closed state (when ATP binds) but become coupled as the channel opens. The finding supports the hypothesis that formation of a tight NBD1/NBD2 dimer is linked to opening of the CFTR channel pore. The use of the evolutionary record for target selection broadens the scope of the experiments and confirms the existence of a common ABC protein coupling mechanism, involving NBD dimerization.

Funded by NIH DK51767, to D.C.G.

*Where applicable, the authors confirm that the experiments described here conform with the Physiological Society ethical requirements.*

---

PC42

**Chloride transport across liposomal membranes by an artificial anionophore**

L.K. Hughes[1], G. Magro[2], J. Joos[2], J.P. Clare[2], A.L. Sisson[2], A.V. Koulov[3], T.N. Lambert[3], R. Shukla[3], M. Jain[3], J. Boon[3], B.D. Smith[3], D.N. Sheppard[1] and A.P. Davis[2]

*[1]Physiology, University of Bristol, Bristol, UK, [2]Chemistry, University of Bristol, Bristol, UK and [3]Department of Chemistry and Biochemistry and Walther Cancer Research Center, University of Notre Dame, Notre Dame, IN, USA*

Small molecules that mimic the action of cation transporters are well known. However, until recently similar molecules that transport anions have been unavailable. In previous work (Koulov *et al.* 2003), we demonstrated that a family of small molecules derived from cholic acid termed 'cholapods' bind anions with high-affinity and promote $Cl^-$ efflux from liposomes. We have also demonstrated that cholapods induce $Cl^-$ transport across MDCK epithelia (Koulov *et al.* 2003) and $Cl^-$-dependent currents in excised inside-out membrane patches. Because electrophysiological studies of cholapods using cells do not distinguish between (i) cholapods themselves mediating anion flow and (ii) cholapods interacting either directly or indirectly with transport proteins to induce current flow, we sought to investigate the transport activity of cholapods in an artificial environment.

To achieve this goal, we modified the technique of Riquelme *et al.* (1990) to study cholapods in excised inside-out membrane patches from giant liposomes synthesised from the phospholipid asolectin by the dehydration/rehydration method. As a control, we studied the cystic fibrosis transmembrane conductance regulator (CFTR) $Cl^-$ channel. To measure $Cl^-$ flow across excised inside-out membrane patches from giant liposomes, we imposed a large $Cl^-$-concentration gradient across the membrane patch (pipette (external) $[Cl^-]$ = 10 mM and bath (internal) $[Cl^-]$ = 147 mM) and clamped voltage at -50 mV.

Like CFTR recorded in cellular membranes, CFTR incorporated into giant liposomes formed $Cl^-$-selective channels regulated by cyclic AMP-dependent phosphorylation and intracellular ATP (n = 3). We then synthesised giant liposomes with no added cell

membrane to study the activity of cholapods in a similar environment. Tetrahydrofuran (THF; 0.24%, v/v), the vehicle used to solubilise cholapods caused no change in current (n = 5). In contrast, addition of the cholapod RS2 (150 μM) to the solution bathing the intracellular side of the excised membrane caused an increase in current from -0.12 + 0.04 pA to -2.43 ± 0.64 pA (n = 3-7; $p < 0.05$, Students t test) that was concentration dependent, but time independent (n = 4). Of note, no unitary events were discernable in the current records. In the presence of symmetrical 147 mM $Cl^-$ solutions, the RS2-induced current had a linear current-voltage relationship with a reversible potential close to 0 mV. We interpret our data to suggest that cholapods mediate $Cl^-$-dependent ion transport across liposomal membranes. Our data also suggest that giant liposomes might prove a useful tool to study both incorporated ion channels and artificial transporters in isolation.

Koulov AV et al. (2003). Angew Chem Int Ed Engl 42, 4931-4933.

Riquelme G et al. (1990). Biochem 29, 11215-11222.

We thank Drs G. Riquelme (University of Chile) and O. Moran (Istituto di Biofisica, Genoa) for their valuable advice. Supported by the BBSRC, CF Trust and EPSRC.

*Where applicable, the authors confirm that the experiments described here conform with the Physiological Society ethical requirements.*